Kinetics Influence of Operation Conditions on Crystal Growth of Calcium Nitrate Tetrahydrate in a Circulating Fluidized Bed

Liu, Dechun*+

School of Materials Science and Engineering, Southwest University of Science and Technology,
Mianyang 621010, Sichuan, P.R. CHINA

Zhu, Jiahua

School of Chemical Engineering, Sichuan University, Chengdu 610021, Sichuan, P.R. CHINA

ABSTRACT:: *In order to improve the traditional freezing crystallization process of calcium nitrate in nitric phosphate process, crystal growth experiments by adding $Ca(NO_3)_2 \cdot 4H_2O$ seeds in supersaturated calcium nitrate solution in a Circulating Fluidized Bed (CFB) crystallizer were carried out on crystal growth kinetics. The results showed that the growth of $Ca(NO_3)_2 \cdot 4H_2O$ crystals is a complicated mass transfer process. The mean mass crystal growth rate (R_G) of $Ca(NO_3)_2 \cdot 4H_2O$ increased linearly with the fluid circulated velocity at fixed relative supersaturation and enlarged with relative supersaturation increasing. The crystallization kinetics follows the first order equation. The overall activation energy and the order of the overall growth kinetics of $Ca(NO_3)_2 \cdot 4H_2O$ crystals were calculated by the isothermal method. The R_G of $Ca(NO_3)_2 \cdot 4H_2O$ crystals remains basically stationary within the entire crystallization time in the CFB crystallizer. The results have a deep significance to exploit a new CFB crystallization process for the production of $Ca(NO_3)_2 \cdot 4H_2O$ crystals instead of the traditional one.*

KEYWORDS: *Circulating Fluidized Bed (CFB); Calcium nitrate tetrahydrate; Mass transfer; Crystal growth rate; Crystal growth kinetics.*

INTRODUCTION

Phosphorus derived from the nitrophosphate rock is an essential element for plant growth and in the world the distribution of phosphate rock sources is concentrated in a small number of countries [1]. As the most major by-products of nitric phosphate manufactured [2], calcium nitrate can be precipitated and separated as stable α-, β-$Ca(NO_3)_2 \cdot 4H_2O$ stable crystals at ambient temperature, which have lower critical suction humidity. With the development of technologies, $Ca(NO_3)_2 \cdot 4H_2O$ can often be used as available calcium filled with nitrogen fertilizer in agriculture, a precursor for the synthesis of hydroxyapatite [3], powders set accelerator for cement at low temperature [4]. Especially, $Ca(NO_3)_2 \cdot 4H_2O$ crystal and its mixture with some other inorganic salts and organic compounds

have a high latent heat of fusion and low melting point, which bring them to be considered the Phase Change Materials (PCMs) for thermal energy storage [5].

However, $Ca(NO_3)_2 \cdot 4H_2O$ easily generates a supersaturated solution. The process of spontaneous crystallization is impossible upon its physical properties. Therefore, the crystallization of calcium nitrate is one of the most complicated processes in the production of calcium nitrate, and there still exist many difficulties in preparing for the calcium nitrate crystallization stage. Normally, the freezing method has been adopted in the production of $Ca(NO_3)_2 \cdot 4H_2O$ crystals, in which the piston pushing centrifuge or the double drum vacuum filter has been used in the following separation of $Ca(NO_3)_2 \cdot 4H_2O$ crystals. Generally speaking, the piston pushing centrifuge has easy abrasive moving parts, poorer stability, and lower washing efficiency. Meanwhile, the double-drum vacuum filter exists a complex structure, multi accessory equipment and higher fluid content in filter cake [6]. Therefore, in order to produce $Ca(NO_3)_2 \cdot 4H_2O$ crystals efficiently, it is required to improve crystal separation process or develop new technology for calcium nitrate production.

Circulating Fluidized Bed (CFB) technology has an excellent mixing efficiency between a carrier fluid and the solid particles [7]. And the suspended solids in CFB can provide a large surface area for the crystal growth [8], which has the advantages of solution crystallization and purification. So CFB technology has been widely used in crystallization industry [9]. Moreover, the crystal growth from circulating fluid is affected by mass transport processes. Although the crystallization of calcium nitrate solution is very difficult and explicates due to the special nature of $Ca(NO_3)_2 \cdot 4H_2O$ crystals, the hydrodynamic conditions of the solution in CFB crystallizer have a direct impact on the crystallization kinetics of $Ca(NO_3)_2 \cdot 4H_2O$ [10,11]. So that the small size of $Ca(NO_3)_2 \cdot 4H_2O$ particles should be grown up in a CFB crystallizer under the seriously controlling of crystallization parameters. Therefore, in order to exploit a newly high-efficient CFB crystallization process for $Ca(NO_3)_2 \cdot 4H_2O$ crystal production instead of the traditional freezing method, in this article, the growth kinetics of $Ca(NO_3)_2 \cdot 4H_2O$ seeds in the supersaturated calcium nitrate solution in the SCFB crystallizer were systematically investigated.

EXPERIMENTAL PROCEDURES

$Ca(NO_3)_2 \cdot 4H_2O$ (monoclinic system [12], density 1.87 g/cm³, AR grade) was produced by a traditional freezing crystallization process from Chengdu Kelong Chemical Reagents Factory, China and was used without further purification.

The mean mass crystal growth rates (R_G) of $Ca(NO_3)_2 \cdot 4H_2O$ crystals were measured in a CFB crystallizer system, which is illustrated in Fig. 1. The crystal growth rates (R_G) and the size distributions of $Ca(NO_3)_2 \cdot 4H_2O$ crystals were measured in a CFB crystallizer system, which is illustrated in Fig. 1. Briefly, the saturated solution of calcium nitrate was prepared in a saturation device (consisting of automatic temperature controlled setup 1, saturator 2 and thermostatic bath 3) and controlled to form a steady circulated fluid flowing by a magnetic pump (4) and rotermeter (7). The relative supersaturation (σ) was produced through heat exchanging when the solution flowed through a condensing apparatus (6). 10 g of vacuum-dried $Ca(NO_3)_2 \cdot 4H_2O$ crystal seeds with the average diameter of 0.278 mm were added into the CFB crystallizer (8, 9 mm of nozzle diameter, 40 mm of diameter with 200 mm length of the bed layer, 80 mm of expanding section diameter in the upper part with 80 mm length, borosilicate glass) after the stabilization of fluid flowing. The temperatures of the saturation device and the bed layer of the CFB crystallizer were read by a mercurial thermometer (5). The grown-up particles of $Ca(NO_3)_2 \cdot 4H_2O$ were taken out from the top of the CFB crystallizer to be dried (vacuum) and weighed, then R_G of $Ca(NO_3)_2 \cdot 4H_2O$ crystals was calculated by Eq. (1) [13].

$$G = \frac{3\alpha L_0}{\beta t} \rho_c \left[\left(\frac{M_i}{M_0} \right)^{\frac{1}{3}} - 1 \right] \tag{1}$$

Here $Ca(NO_3)_2 \cdot 4H_2O$ crystals were supposed to be a spherical particle. α and β are the volume and area shape factors, respectively. Although, $Ca(NO_3)_2 \cdot 4H_2O$ crystals belong to the monoclinic system and have unequal values, the value of α/β is closer to 1/6.

Meanwhile, in order to obtain the experimental required relative supersaturation (σ) in the CFB crystallizer, it is very essential to determine the solubility of $Ca(NO_3)_2 \cdot 4H_2O$ crystal in the CFB crystallizer. The initially saturated solubility of calcium nitrate was prepared according to the solubility data in the literature [14],

Table 1: The solubility and relative supersaturation of calcium nitrate solution at 0-40 ℃ in a CFB crystallizer.

$T/$(℃)	0	5	10	15	20	25	30	35	40
Solubility/(g solute/100 g water)	102	106.46	115	122.7	129	138	149	163.83	189
σ (ΔT=15 ℃)	0.20	0.21	0.20	0.21	0.27	0.37			
σ (ΔT=10 ℃)	0.13	0.15	0.12	0.12	0.16	0.19	0.27		
σ (ΔT=5 ℃)	0.04	0.08	0.07	0.05	0.07	0.08	0.10	0.15	
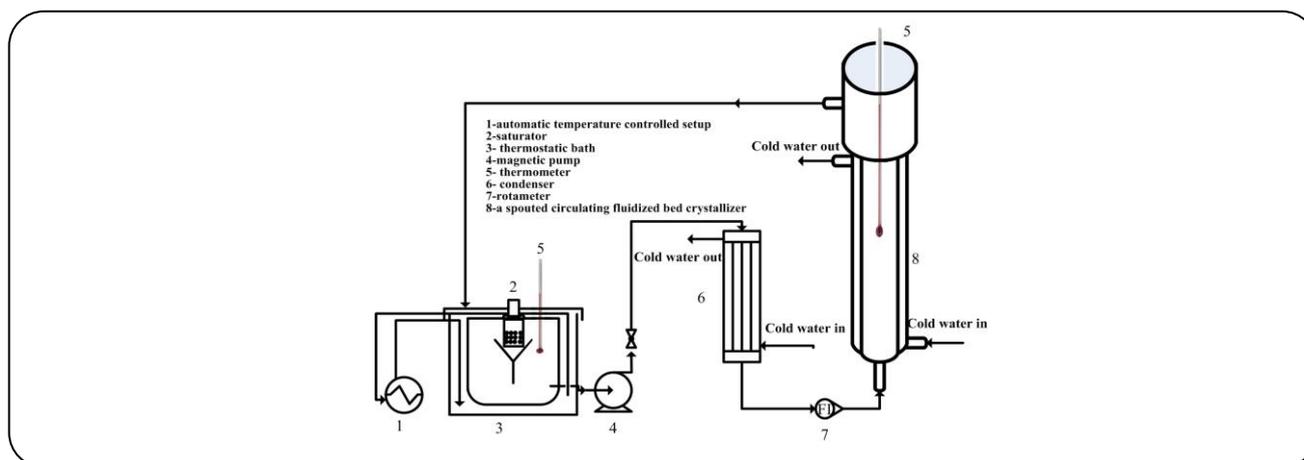
Fig. 1: Schematic diagram of the experimental setup.

and the measurement results were shown in Table 1. Therefore, the relative supersaturation (σ) of the calcium nitrate solution required for the entire crystallization experiments in CFB was prepared according to the data determined above.

RESULTS AND DISCUSSION
Influence of fluid circulating velocity

Due to the fluid flowing condition in a CFB is a turbulent flow [15], the mass transfer between the solution and $Ca(NO_3)_2 \cdot 4H_2O$ seeds can be definitely enhanced, resulting in the growth rate of $Ca(NO_3)_2 \cdot 4H_2O$ crystals accelerated. Therefore, the R_G of $Ca(NO_3)_2 \cdot 4H_2O$ crystals in the CFB crystallizer is seriously affected by fluid circulated velocity in the CFB crystallizer, and the results are shown in Fig. 2 under crystallization conditions of σ=0.07, at 21℃ and 30 min. It is found that R_G values of $Ca(NO_3)_2 \cdot 4H_2O$ crystals increased with fluid circulated velocities of the CFB crystallizer under the same supersaturation. It demonstrates that the growth of $Ca(NO_3)_2 \cdot 4H_2O$ crystals in a circulated flowing solution is mainly influenced by the mass transfer process. This is because of the hydrodynamic conditions of solution

in the CFB crystallizer have a direct impact on the crystallization kinetics of $Ca(NO_3)_2 \cdot 4H_2O$ [16], so the diffused mass rates between the supersaturated solution and $Ca(NO_3)_2 \cdot 4H_2O$ crystal particles were enhanced with increasing fluid circulated velocity, which resulted in R_G value enlarged.

Influence of relative supersaturation and temperature on the growth of $Ca(NO_3)_2 \cdot 4H_2O$ crystals

Crystallization in the CFB crystallizer is a very complex operation. According to the physical and chemical properties of calcium nitrate, in a supersaturated solution in the CFB crystallizer, the main mass transfer mechanism is the diffusion of solute to the surface of $Ca(NO_3)_2 \cdot 4H_2O$ crystals, which follows by the adsorption of solute on the surface and integrates of the solute to the crystal structure [13]. Therefore, some empirical equations can be used to calculate the crystal growth rate, if the over-all driving force of crystal growth is expressed as relative supersaturation (σ), the total crystal growth rate of the semi-empirical equation can be written as follows [17,18]:

$$R_G = K_G \sigma^n \qquad (2)$$

If K_G can be expressed as an Arrhenius-type equation with temperature (T):

$$K_G = K_0 \exp\left(-\frac{E_A}{RT}\right) \qquad (3)$$

The above expression is substituted into the formula (2) and then by a logarithm for Kelvin temperature T, Eq. (4) can be obtained:

$$\frac{\partial \ln R_G}{\partial (1/T)} = -\frac{E_A}{R} + \ln \sigma \frac{\partial \ln n}{\partial (1/T)} \qquad (4)$$

Therefore, the influence of the temperature on R_G values of Ca(NO$_3$)$_2$·4H$_2$O crystals can be typically plotted by the form of Eq. (4). The values of E_A and n may be gained.

The evolutions of R_G values of Ca(NO$_3$)$_2$·4H$_2$O with relative supersaturation (σ) of the solution under different temperatures at fixed crystallization conditions of u_0=0.012 m/s and 0.5 h are shown in Fig. 3. The experimental data showed that the crystal growth rate was increasing with both relative supersaturation and temperature and fit with the semi-empirical relation given in Eq. (2) by an isothermal method, and the fitting results were shown in Table 2. Meanwhile, by a logarithm for Eq. (3), then obtained:

$$\frac{\partial \ln K_G}{\partial (1/T)} = -\frac{E_A}{R} \qquad (5)$$

From Eq. (5), the higher of E_A, the influence of T is stronger on K_G, and they are positively ratios. And the representation of the logarithm of K_G against $1/T$ provides a straight line with $-E_A/R$. The square block points in Fig. 4 illustrate this behavior for the crystal growth rate constants obtained at 15, 18, 21 and 25 ℃ (curve a). The estimated E_A was 19.4 kJ·mol^{-1} for temperatures below 25 ℃. According to Eq. (4) and (5), if the reaction order of overall growth kinetics (n) was constant within all ranges of crystal temperature, so that $\partial \ln K_G / \partial (1/T)$ =-2327.9 K、 $\partial \ln R_G / \partial (1/T)$ =-282.3 K, and $\partial \ln n / \partial (1/T)$ =-865.9 K from Fig. 4 (curves of a and b). According to the functional relation between $\ln K_G$, $\ln R_G$, and $1/T$, n can be calculated roughly [19], here the one was to increase from about 0.1 to 0.21 with temperature from 15 to 25 ℃. This demonstrates that the R_G of Ca(NO$_3$)$_2$·4H$_2$O seeds is severely affected by the crystallization temperature.
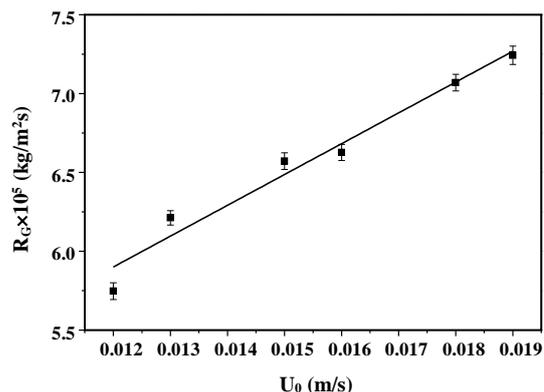
Fig. 2: Influence of the fluid circulated velocity in a CFB crystallizer on R_G of Ca(NO₃)₂·4H₂O. (conditions: the total circulating fluid volume is 3000 ml，the saturation temperature is at 25 •C, the crystal temperature is at 21•C and the crystal time lasts 30 min).
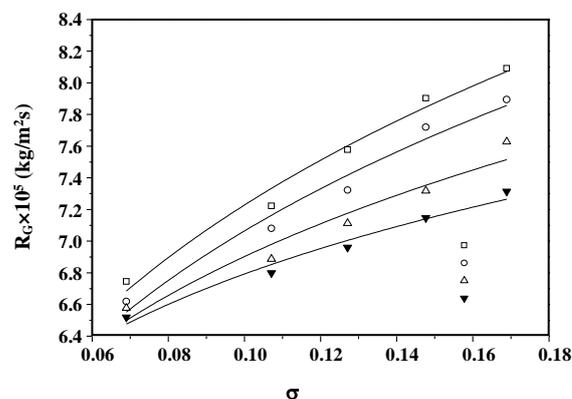
Fig. 3: R_G values of Ca(NO₃)₂·4H₂O measured by the isothermal method at different temperatures.
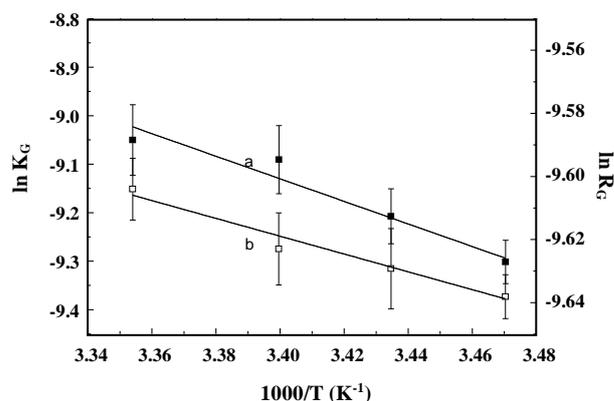
Fig. 4: Effect of the inverse of temperature on the K_G (curve a) and on the R_G inferred at σ=0.07 (curve b).

Table 2: Parameters of equation (3) that best fit the experimental results presented in Fig. 3.

T/°C	$K_G/(kg/m^2 \cdot s) \cdot (kg/m^3)^{-n}$	n	R^2
25	1.17379×10^{-4}	0.21055	0.97686
21	1.12721×10^{-4}	0.20292	0.96497
18	1.00280×10^{-4}	0.16221	0.93233
15	9.12758×10^{-5}	0.12832	0.96775
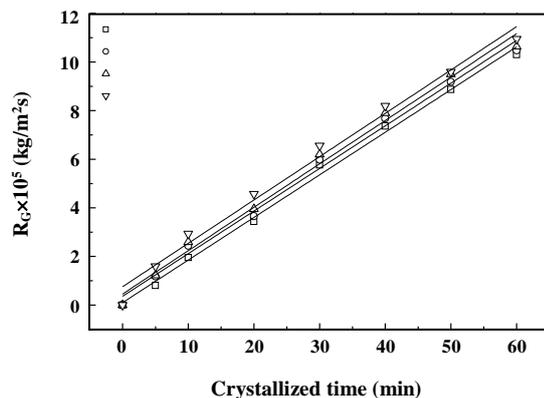
Fig. 5: Relation between crystal growth kinetics versus reaction time.

The crystal growth kinetics of $Ca(NO_3)_2 \cdot 4H_2O$ seeds in the CFB crystallizer

Fig. 5 shows the kinetics development curves between R_G of $Ca(NO_3)_2 \cdot 4H_2O$ crystals and fluid circulated velocity in the CFB crystallizer with at 21°C and $\sigma = 0.07$. It is found that the kinetics curves of different circulating fluid flowing velocities had an identical variation tendency under the same relative supersaturation. After linear fitting, the first-order crystallization kinetic equation was gained. In comparison with the traditional freezing crystallization process, the crystal growth circumstance in the CFB crystallizer is fairly stable and uniform, resulting in a larger R_G of $Ca(NO_3)_2 \cdot 4H_2O$ crystals and bigger crystals with a preferably regular shape (see Fig. 6). The results demonstrate that the R_G of $Ca(NO_3)_2 \cdot 4H_2O$ crystals in the CFB crystallizer can sustain a constant value and is affected seriously by fluid circulated velocity, crystallization time and other factors [20].

CONCLUSIONS

Through a series of experiments on the growth of $Ca(NO_3)_2 \cdot 4H_2O$ seeds added into calcium nitrate supersaturating solution, the crystal growth rates of $Ca(NO_3)_2 \cdot 4H_2O$ crystals in CFB crystallizer were determined. And the hydrodynamics of the successful growth of $Ca(NO_3)_2 \cdot 4H_2O$ seeds in the CFB crystallizer were discussed. Simultaneously, a crystal growth empirical model was developed to interpret the effects of crystallization operating conditions on the crystallization kinetics of $Ca(NO_3)_2 \cdot 4H_2O$ in CFB crystallizer. It is shown that R_G increased with the circulating fluid flow velocity under the same relative supersaturation and with relative supersaturation at fixed the same operating velocity. And the first-order crystallization kinetic equation was gained. By an isothermal method, the apparent activation energy and the order of overall growth kinetics were calculated with the crystal growth data of $Ca(NO_3)_2 \cdot 4H_2O$ seeds at 15, 18, 21 and 25 °C in the CFB crystallizer. And R_G of $Ca(NO_3)_2 \cdot 4H_2O$ crystals in CFB remained constant at entire crystal times. The results indicate that the growth of $Ca(NO_3)_2 \cdot 4H_2O$ crystals in the CFB crystallizer is a complicated mass transfer process and suffers seriously from numerous crystallization factors, and the efficient CFB crystallization technology is a great substitute for the traditional freezing crystallization process of calcium nitrate.

Acknowledgments

Nomenclature

R_G	Mean mass crystal growth rate, $kg/m^2 \cdot s$
ρ_c	Seed density, $1870 \, kg/m^3$
M_0	Seed mass, kg
σ	$=(c-c^*)/c^*$, relative supersaturation
K_G	Crystal growth constant, $(kg/m^2 \cdot s)(kg/m^3)^{-n}$
n	Order of overall growth kinetics
T	The crystallization temparature, K
R^2	The correlation coefficient
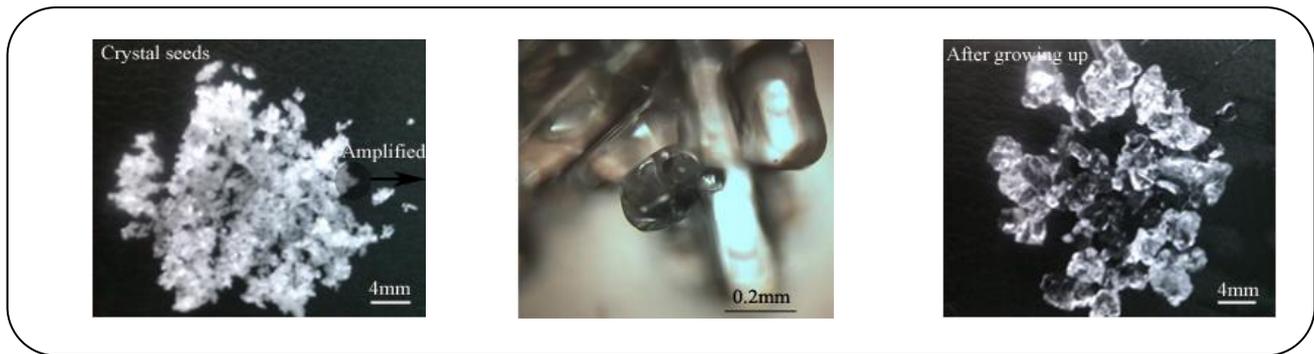
Fig. 6: The macroscopic crystal morphologies of Ca(NO₃)₂·4H₂O seeds and typical grown-up sample in the SCFB crystallizer (conditions: at 21℃, u₀=0.012 m/s and σ = 0.07 for 2.5 h).

c^*	Saturation concentration, kg/kg
L0	Seed crystal size, 0.278 mm
Mi	Crystal growth mass, kg
t	Crystallization time, min
u0	Fluid circulated velocity, m/s
K0	The pre-exponential factor
EA	The overall activation energy, kJ/mol
R	Gas constant, J/mol·K
c	Concentration, kg/kg

REFERENCES

[1] Cooper J., Lombardi R., Boardman D., Carliell-Marquet C., The Future Distribution and Production of Global Phosphate Rock Reserves, *Resour. Conserv. Recy.,* **57**: 78-86 (2011).

[2] Abdel-aal E. A. and Amer A. M., Evaluation of Sebaiya-west Phosphate Concentrate for Nitrophosphate Fertilizer Production, *Miner. Eng.*, **8**: 1221-1230 (1995).

[3] Dos Santos M.L., Riccardi C.S., Noronha A.L., Filho Edson de A., Olyveira Gabriel M., Guastaldi A.C., Influence of Aging Time of the Sol on the Synthesis of Hydroxyapatite Powders Using Ca(NO₃)₂·4H₂O and H₃PO₄ as Precursors, *Mater. Focus*, **4**: 189-192 (2015).

[4] Justnes H., Nygaard E.C., Technical Calcium Nitrate as Set Accelerator for Cement at Low Temperatures, *Cement Concrete Res.*, **25**: 1766-1774 (1995).

[5] Gadzuric S., Vranes M., Dozic S., Electrical Conductivity and Phase Transitions of Calcium Nitrate+Ammonium Nitrate+Water Mixtures, *J. Chem. Eng. Data*, **55**: 1990-1993 (2010).

[6] Cheng G.H., Separation of Calcium Nitrate Crystals in Nitrophosphate Process, *Phosphate and Compound Fertilizer*, **16**: 2-4 (2001).

[7] Wang S.Y., Yang X., Lu H.L., Yu L., Wang S., Ding Y.L., CFD Studies on Mass Transfer of Gas-to-particle Cluster in a Circulating Fluidized Bed, *Comput. Chem. Eng.*, **33**: 393-401 (2009).

[8] Wan L., Alvarez-Cuenca M., Upreti S.R., Lohi A., Development of a Three-phase Fuidized Bed Reactor with Enhanced Oxygen Transfer, *Chem. Eng. Process.*, **49**: 2-8 (2010).

[9] Su C.C., Fan C.C., Anotai J., Lu M.C., Effect of the Iron Oxide Catalyst on *o*-toluidine Oxidation by the Fluidized-bed Fenton Process, *Environ. Technol.*, **35**: 89-94 (2014). .

[10] Mazumder J., Zhu J. X., Ray A.K., Optimal Design of Liquid–Solid Circulating Fluidized Bed for Continuous Protein Recovery, *Powder Technol.*, **199**: 32-47 (2010).

[11] Binev D., Seidel-Morgenstern A., Lorenz H., Study of Crystal Size Distributions in a Fluidized Bed Crystallizer, *Chem. Eng. Sci.*, **33**: 116–124 (2015).

[12] Frazier A.W., Mullins R.C., Smith J.P., Fertilizer Materials, Crystallography of Hydrates of Calcium Nitrate, *J. Agric. Food Chem.*, **12**: 478-479 (1964).

[13] Sahin Ö., Özdemir M., Kendirci H.,d Bulutcu A.N., Determination of Growth and Dissolution Mass Rate of Boric Acid Crystals by a Simple Computer Program, *J. Cryst. Growth*, **219**: 75-82 (2000).

[14] Taylor H.S., Hrndbre W.N., The Solubility Curves of Salt Hydrates: Calcium Nitrate, *J. Am. Chem. Soc.*, **37**: 1688-1694 (1915).

[15] Martins P.M., Rocha F.A., The Role of Diffusional Resistance on Crystal Growth: Interpretation of Dissolution and Growth Rate Data, *Chem. Eng. Sci.*, **61**: 5686-5695 (2006).

[16] Binev D., Seidel-Morgenstern A., Lorenz H., Study of Crystal Size Distributions in a Fluidized Bed Crystallizer, *Chem. Eng. Sci.*, **33**:116-124 (2015).

[17] Garside J., The Concept of Effectiveness Factors in Crystal Growth, *Chem. Eng. Sci.,* **26**: 1425–1431 (1971).

[18] Kumar K.V., Regression Analysis for the Two-Step Growth Kinetics of Crystals in Pure Solutions, *Ind. Eng. Chem. Res.*, **48**: 7852-7859 (2009).

[19] Martins P. M. and Rocha F. A., Kinetic Studies on the Influence of Temperature and Growth rate History on Crystal Growth, *Cryst. Res. Technol.*, **43**: 1258-1267 (2008).

[20] Clifford Y.T., Chen P.C., Tsao T.M., Growth Kinetics of CaF_2 in a pH-Stat Fluidized-Bed Crystallizer, *J. Cryst. Growth*, **290**: 576–584 (2006).